Journal of Chemical Health Risks

www.jchr.org

JCHR (2026) 16(3), 268-275 | ISSN:2251-6727

# Photocatalytic degradation of Methylene Blue dye using $CaFe_2O_4$/SWCNT Nanocomposite

**Mehtab Singh Sidhu[1], Vijay Anand[1*]**

1- Department of Prosthodontics, Saveetha Dental College and Hospitals, Saveetha Institute of Medical & Technical Sciences, Saveetha University, Chennai 600077, Tamil Nadu, India

*(Received: 16 March 2026 Revised: 14 April 2026 Accepted: 01 May 2026)*

**KEYWORDS**

$CaFe_2O_4$/SWCNT nanocomposite; Photocatalysis; Methylene blue degradation; Wastewater treatment; Nanocomposite catalyst

**ABSTRACT:**

**Introduction**: The discharge of dye-containing wastewater from textile and related industries poses serious environmental concerns due to the toxicity, persistence, and non-biodegradable nature of synthetic dyes. Among these pollutants, methylene blue (MB) is widely used and frequently detected in industrial effluents. Photocatalysis has emerged as an effective and eco-friendly approach for dye degradation. In this context, ferrite/carbon nanocomposites have gained attention because of their enhanced charge separation and catalytic efficiency.

**Objectives**: This study aimed to synthesize a $CaFe_2O_4$/SWCNT nanocomposite and evaluate its photocatalytic performance for the degradation of methylene blue dye under UV irradiation

**Methods**: The $CaFe_2O_4$/SWCNT nanocomposite was synthesized by a hydrothermal-assisted method followed by calcination. The prepared material was characterized using UV–Visible spectroscopy and FTIR analysis to examine optical properties and functional groups. Photocatalytic degradation experiments were carried out using 10 mg of catalyst dispersed in 100 mL of 10 ppm MB solution under UV light irradiation. The degradation process was monitored at 662 nm using UV–Visible spectroscopy. Degradation efficiency and pseudo-first-order kinetic behavior were determined.

**Results**: UV–Visible analysis showed enhanced light absorption and broadened spectral response for the $CaFe_2O_4$/SWCNT nanocomposite compared with pristine SWCNT. FTIR spectra confirmed the presence of characteristic Fe–O/Ca–O bonds and carbon functional groups, indicating successful composite formation. The photocatalyst achieved 79.9% degradation of MB within 120 min, while only 8.9% degradation was observed under light-only conditions. The degradation followed pseudo-first-order kinetics with a rate constant of 0.01005 $min^{-1}$, which was significantly higher than the control (0.00078 $min^{-1}$).

**Conclusion**: The $CaFe_2O_4$/SWCNT nanocomposite exhibited excellent photocatalytic activity toward methylene blue degradation due to improved light absorption, efficient charge separation, and enhanced radical generation. The results demonstrate that this material is a promising low-cost photocatalyst for wastewater treatment and environmental remediation applications.

## 1. Introduction

Rapid industrialization and urban expansion have led to the continuous discharge of dye-containing wastewater into aquatic environments. Synthetic dyes released from textile, paper, printing, cosmetic, and pharmaceutical industries are among the most problematic contaminants because of their complex aromatic structures, high chemical stability, and resistance to biodegradation [1,2]. Even at low concentrations, dyes reduce light penetration in water bodies, disturb photosynthetic activity, and may generate toxic, mutagenic, or carcinogenic by-products during natural decomposition processes [3]. Therefore, the development of efficient, economical, and environmentally benign technologies for dye removal has become a major research priority.Among the various organic pollutants, Methylene Blue (MB) is widely employed as a model cationic dye in photocatalytic studies due to its intense color, well-defined absorption peak, and persistence in aqueous media [4]. MB is commonly used in textile dyeing, paper coloring, and medical applications; however, excessive exposure can cause irritation, respiratory distress, nausea, and ecological toxicity [5]. Conventional wastewater treatment methods such as adsorption, coagulation, membrane filtration, and biological treatment often suffer from incomplete mineralization, secondary sludge generation, high operational cost, or poor effectiveness

Journal of Chemical Health Risks
www.jchr.org
JCHR (2026) 16(3), 268-275 | ISSN:2251-6727

toward stable dye molecules [6]. In contrast, semiconductor-based photocatalysis has emerged as an advanced oxidation process capable of converting organic contaminants into harmless products such as $CO_2$, $H_2O$, and inorganic ions under light irradiation [7].Photocatalysis relies on the generation of electron-hole pairs when a semiconductor absorbs photons with energy equal to or greater than its band gap. These photogenerated charge carriers migrate to the catalyst surface and react with adsorbed oxygen or water molecules to produce highly reactive species such as hydroxyl radicals (•OH), superoxide radicals ($\bullet O_2^-$), and singlet oxygen, which oxidize dye molecules efficiently [8]. However, practical application of many traditional photocatalysts, especially $TiO_2$ and ZnO, is restricted by wide band gaps, rapid recombination of charge carriers, and low utilization of visible light, which constitutes the major fraction of solar radiation [9]. Consequently, visible-light-active magnetic ferrite photocatalysts have attracted increasing attention. Among ferrite semiconductors, calcium ferrite ($CaFe_2O_4$) is a promising p-type oxide semiconductor owing to its narrow band gap (~1.8–2.1 eV), strong visible-light absorption, chemical stability, low toxicity, and earth-abundant constituents [10,11]. $CaFe_2O_4$ has been investigated for photocatalytic degradation of dyes, water splitting, sensors, and energy storage applications. Its orthorhombic crystal structure and suitable valence/conduction band positions enable the generation of reactive oxygen species under visible light irradiation [12]. In addition, the magnetic nature of ferrites can facilitate catalyst recovery and reuse, which is highly desirable for wastewater treatment processes. Nevertheless, pristine $CaFe_2O_4$ often exhibits drawbacks such as low specific surface area, particle agglomeration, and fast recombination of photogenerated electrons and holes, resulting in moderate photocatalytic performance [13]. To overcome these limitations, coupling ferrite semiconductors with carbonaceous nanomaterials has become an effective strategy. Carbon nanotubes (CNTs), especially single-walled carbon nanotubes (SWCNTs), possess extraordinary electrical conductivity, large aspect ratio, high mechanical strength, and large specific surface area [14]. SWCNTs can act as electron acceptors and conductive pathways, promoting rapid transfer of photogenerated electrons away from the semiconductor surface and suppressing electron-hole recombination. Their tubular nanostructure also provides abundant adsorption sites for dye molecules through π–π interactions and electrostatic attraction, thereby increasing local pollutant concentration near active catalytic sites [15]. The formation of a $CaFe_2O_4$/SWCNT nanocomposite is therefore expected to generate significant synergistic effects. First, intimate interfacial contact between $CaFe_2O_4$ nanoparticles and SWCNTs can improve charge separation and carrier mobility. Second, the dispersion of $CaFe_2O_4$ on SWCNT networks can reduce nanoparticle aggregation and expose more reactive surface sites. Third, enhanced adsorption of MB onto SWCNT surfaces can accelerate interfacial oxidation reactions. Finally, the composite may exhibit broader light absorption and improved structural stability during repeated photocatalytic cycles [16]. Similar improvements have been reported for ferrite/CNT-based heterostructures, where CNT incorporation markedly enhanced degradation rates of dyes and other organic pollutants under visible light [17,18]. The photocatalytic degradation of MB using $CaFe_2O_4$/SWCNT nanocomposites generally involves adsorption of dye molecules on the catalyst surface followed by light-induced excitation of $CaFe_2O_4$. The excited electrons are transferred to SWCNTs, where they react with dissolved oxygen to form $\bullet O_2^-$ radicals, while holes remaining in the valence band oxidize water or hydroxide ions to generate •OH radicals. These reactive species attack the chromophoric structure of MB, leading to successive N-demethylation, ring opening, and eventual mineralization [19]. Because SWCNTs serve as electron sinks, the lifetime of charge carriers is prolonged, resulting in superior photocatalytic activity compared with bare $CaFe_2O_4$. In this context, the present manuscript focuses on the synthesis, characterization, and photocatalytic application of a $CaFe_2O_4$/SWCNT nanocomposite for the degradation of Methylene Blue dye in aqueous solution. The study aims to evaluate how SWCNT incorporation influences structural, optical, and morphological properties of $CaFe_2O_4$, as well as its photocatalytic efficiency, kinetics, and reusability. The findings are expected to provide valuable insight into designing high-performance ferrite/carbon hybrid photocatalysts for sustainable wastewater remediation.

## 2. Objectives

The primary objective of this study was to synthesize a $CaFe_2O_4$/SWCNT nanocomposite and investigate its potential as an efficient photocatalyst for the degradation of methylene blue dye in aqueous solution under UV irradiation. The study further aimed to characterize the optical and functional properties of the prepared nanocomposite using UV–Visible and FTIR techniques, evaluate its photocatalytic degradation efficiency and

Journal of Chemical Health Risks
www.jchr.org
JCHR (2026) 16(3), 268-275 | ISSN:2251-6727

reaction kinetics, and understand the synergistic role of SWCNT in enhancing charge separation, light absorption, and overall catalytic performance. Ultimately, the work sought to develop a low-cost and effective nanocomposite material for wastewater treatment and environmental remediation applications.

## 3. Methods

### 3.1 Chemicals and Reagents

Analytical-grade iron(III) nitrate nonahydrate ($Fe(NO_3)_3 \cdot 9H_2O$), calcium nitrate hydrate ($Ca(NO_3)_2 \cdot xH_2O$), ammonium fluoride ($NH_4F$), ammonium hydroxide ($NH_4OH$), single-walled carbon nanotubes (SWCNTs), and methylene blue (MB) dye were procured from standard chemical suppliers and used without further purification. Deionized water (18.2 MΩ·cm) was used for all solution preparations. Ethanol was employed during the washing process. All reagents used in this study were of analytical grade.

### 3.2 Synthesis of $CaFe_2O_4$/SWCNT Nanocomposite

The $CaFe_2O_4$/SWCNT nanocomposite was synthesized via a hydrothermal-assisted method followed by thermal treatment. Initially, 10 g of $Fe(NO_3)_3 \cdot 9H_2O$ and 3 g of $Ca(NO_3)_2 \cdot xH_2O$ were dissolved separately in deionized water and then mixed under continuous magnetic stirring at 500 rpm to form a homogeneous precursor solution. Subsequently, 2.7 g of $NH_4F$ was added slowly to the solution as a mineralizing and morphology-controlling agent.

After complete dissolution, ammonium hydroxide ($NH_4OH$) was introduced dropwise until the pH of the mixture reached approximately 10, resulting in the formation of a reddish-brown suspension. Separately, an appropriate amount of SWCNT was dispersed in deionized water by ultrasonication for 30 min to achieve uniform dispersion and minimize agglomeration. The dispersed SWCNT suspension was then added to the precursor mixture and stirred continuously for 1 h to ensure intimate interaction between $Ca^{2+}$/$Fe^{3+}$ ions and the nanotube surface.

The resulting suspension was transferred into a Teflon-lined stainless-steel autoclave and maintained at 180 °C for 12 h under autogenous pressure. After completion of the hydrothermal reaction, the autoclave was allowed to cool naturally to room temperature. The obtained precipitate was collected by centrifugation, washed repeatedly with deionized water and ethanol to remove residual ions and impurities, and dried in a hot-air oven at 80 °C for 12 h.

Finally, the dried product was calcined in a muffle furnace at 500 °C for 3 h to improve crystallinity and obtain the final $CaFe_2O_4$/SWCNT nanocomposite powder.

### 3.3 Preparation of Pure $CaFe_2O_4$

For comparison purposes, pristine $CaFe_2O_4$ was synthesized using the same procedure described above, but without the addition of SWCNT. The obtained powder was similarly washed, dried, and calcined under identical conditions.

### 3.4 Characterization Techniques

The structural, functional, and optical properties of the synthesized materials were characterized using standard analytical techniques.

- UV–Visible spectroscopy was carried out in the wavelength range of 200–1000 nm to investigate the optical absorption behavior of SWCNT and $CaFe_2O_4$/SWCNT nanocomposite.
- Fourier transform infrared spectroscopy (FTIR) was performed in the range of 4000–500 $cm^{-1}$ to identify functional groups and bonding interactions in the composite.
- X-ray diffraction (XRD) analysis may be used to determine the crystalline phase and structural purity of the prepared samples.
- Scanning electron microscopy (SEM) and/or transmission electron microscopy (TEM) may be employed to examine surface morphology, particle size, and dispersion of $CaFe_2O_4$ over the SWCNT network.
- Energy-dispersive X-ray spectroscopy (EDX) may be used to confirm elemental composition.

### 3.5 Photocatalytic Degradation of Methylene Blue

The photocatalytic activity of the synthesized $CaFe_2O_4$/SWCNT nanocomposite was evaluated by degradation of methylene blue (MB) dye under UV light irradiation. A UV–Vis lamp with an excitation wavelength corresponding to the absorption region of MB (λ = 662 nm, photon energy = 3.13 eV) was used as the irradiation source. All experiments were conducted at room temperature under ambient conditions.

Journal of Chemical Health Risks
www.jchr.org
JCHR (2026) 16(3), 268-275 | ISSN:2251-6727

In a typical experiment, 10 mg of photocatalyst was dispersed in 100 mL of 10 ppm MB aqueous solution. Prior to light irradiation, the suspension was magnetically stirred in the dark for 30 min to establish adsorption–desorption equilibrium between the catalyst surface and dye molecules.

The reaction mixture was then exposed to UV light under continuous stirring. At predetermined irradiation times (15, 30, 45, 60, 75, and 120 min), aliquots were withdrawn and centrifuged to remove suspended catalyst particles. The residual concentration of MB was determined using a UV–Visible spectrophotometer by monitoring the maximum absorbance peak at 662 nm.

The degradation efficiency (%) was calculated using:

$$\text{Degradation (\%)} = \frac{C_0 - C_t}{C_0} \times 100$$

where:
$C_0$= initial concentration of MB solution
$C_t$= concentration of MB after irradiation time $t$

### 3.6 Kinetic Analysis

The kinetics of photocatalytic degradation were analyzed using the pseudo-first-order Langmuir–Hinshelwood model:

$$\ln\left(\frac{C_0}{C_t}\right) = kt$$

where:
$k$= apparent rate constant ($min^{-1}$)
$t$= irradiation time (min)

The slope of the linear plot of $\ln(C_0/C_t)$ versus time was used to determine the reaction rate constant for both catalytic and light-only systems.

### 3.7 Control Experiment

To evaluate the contribution of direct photolysis, a control experiment was performed under identical irradiation conditions in the absence of photocatalyst (light only). The degradation efficiency obtained from this experiment was compared with that of the catalytic system.

## 4. Results

### 4.1 UV–Visible Spectral Analysis

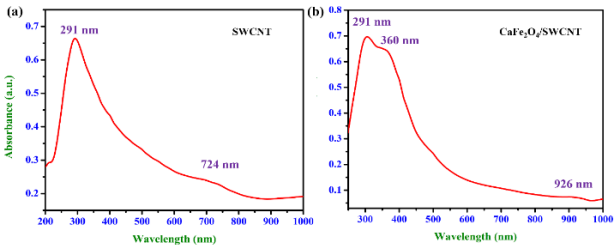


**Figure 1. UV spectroscopy of (a) SWCNT (b) $CaFe_2O_4$/SWCNT Nanocomposite**

The optical absorption properties of pristine SWCNT and the synthesized $CaFe_2O_4$/SWCNT nanocomposite were investigated using UV–Visible spectroscopy in the wavelength range of 200–1000 nm. The UV–Vis spectrum of SWCNT exhibited a prominent absorption peak at 291 nm, which is attributed to the $\pi \rightarrow \pi^*$ electronic transition of the conjugated $sp^2$ carbon network present in the nanotube structure. This characteristic peak confirms the graphitic framework and electronic delocalization of SWCNT.

In the case of the $CaFe_2O_4$/SWCNT nanocomposite, the absorption peak at 291 nm was retained, indicating preservation of the nanotube structure after composite formation. Additionally, a new absorption band was observed at 360 nm, corresponding to charge-transfer transitions involving $Fe^{3+}$–$O^{2-}$ in the $CaFe_2O_4$ lattice or band-to-band excitation of the ferrite semiconductor. A broad absorption tail extending into the visible and near-infrared region with a feature around 926 nm was also observed.

### 4.2 FTIR Analysis

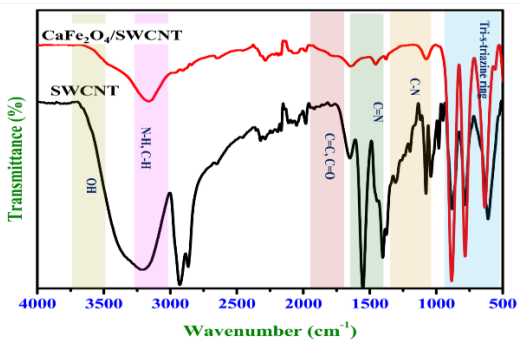


**Figure 2. FTIR analysis of photocatalytic material**

Journal of Chemical Health Risks
www.jchr.org
JCHR (2026) 16(3), 268-275 | ISSN:2251-6727

FTIR spectroscopy was performed to identify the functional groups and confirm the chemical interaction between $CaFe_2O_4$ and SWCNT in the nanocomposite. The FTIR spectrum of pristine SWCNT displayed a broad absorption band in the region of 3400–3600 $cm^{-1}$, corresponding to O–H stretching vibrations of surface hydroxyl groups and adsorbed moisture. These hydroxyl groups are important for photocatalytic processes because they can participate in the formation of hydroxyl radicals during irradiation.

The peaks observed near 2920–3000 $cm^{-1}$ were assigned to C–H stretching vibrations, while the band around 1600–1700 $cm^{-1}$ was attributed to C=C skeletal vibrations of graphitic carbon and/or C=O stretching of oxidized surface groups. Additional bands in the region of 1000–1500 $cm^{-1}$ correspond to C–N, C–O, or aromatic carbon vibrations.

For the $CaFe_2O_4$/SWCNT nanocomposite, these characteristic carbon-related peaks were retained with slight shifts and reduced intensity, indicating strong interaction between the ferrite phase and SWCNT surface. Most importantly, new bands appearing in the low-frequency region of 500–600 $cm^{-1}$ were assigned to Fe–O and Ca–O lattice vibrations of $CaFe_2O_4$. The presence of these metal–oxygen bands confirms successful formation of the ferrite phase within the composite.

### 4.3 Photocatalytic Degradation of Methylene Blue

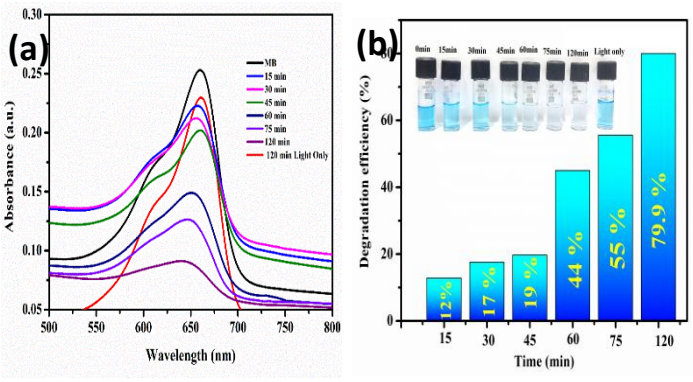


**Figure 3.** ***(a)*** **UV–Vis absorption spectra of methylene blue (MB) at different irradiation times, showing a gradual decrease in absorbance with time.** ***(b)*** **Degradation efficiency (%) of MB as a function of time, along with corresponding photographs showing the color change of the solution.**

The photocatalytic performance of the synthesized $CaFe_2O_4$/SWCNT nanocomposite was evaluated through degradation of methylene blue (MB) dye under UV irradiation. The degradation process was monitored by recording the UV–Visible absorption spectra of MB solution at different irradiation times.

The initial MB solution exhibited a strong absorption peak at 662 nm, corresponding to the chromophoric structure of the dye molecule. Upon exposure to UV light in the presence of the $CaFe_2O_4$/SWCNT catalyst, the intensity of this peak gradually decreased with increasing irradiation time from 15 to 120 min. This continuous reduction in absorbance confirms progressive decomposition of MB molecules in solution. The absence of new significant absorption peaks during irradiation suggests that the dye underwent oxidative degradation rather than conversion into stable colored intermediates. After 120 min of irradiation, the absorbance was drastically reduced, indicating effective dye removal. Visual observation of the reaction solution further supported the spectroscopic results. The intense blue color of MB gradually faded with irradiation time and became nearly colorless after prolonged exposure, confirming decolorization and degradation of the dye. The degradation efficiency of MB was calculated using the concentration ratio before and after irradiation. The results showed a clear increase in degradation percentage with irradiation time. The degradation profile indicates an initial slower stage during the first 45 min, which may be attributed to adsorption–desorption equilibrium and gradual generation of reactive radicals on the catalyst surface. Beyond 45 min, the degradation rate increased markedly, suggesting that sufficient active species were generated to accelerate oxidation of MB molecules.

### 4.4 Effect of Catalyst: Comparison with Light-Only System

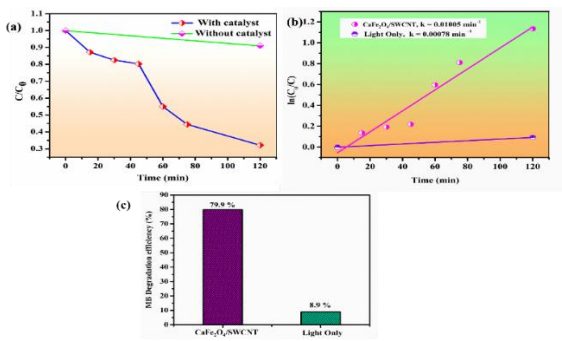


**Figure 4.** ***(a)*** **Variation of normalized concentration ($C/C_0$) of methylene blue (MB) with time in the**

Journal of Chemical Health Risks
www.jchr.org
JCHR (2026) 16(3), 268-275 | ISSN:2251-6727

**presence and absence of $CaFe_2O_4$/SWCNT catalyst. *(b)* Pseudo-first-order kinetic plot of ln($C_0$/C) versus time under catalytic and light-only conditions. *(c)* Comparison of MB degradation efficiency (%) for $CaFe_2O_4$/SWCNT and light-only systems.**

To evaluate the actual contribution of the photocatalyst, a control experiment was conducted under identical UV irradiation conditions without catalyst. In the absence of $CaFe_2O_4$/SWCNT, only 8.9% degradation of MB was observed after 120 min.

In contrast, the catalytic system achieved 79.9% degradation under the same conditions. This substantial difference confirms that direct photolysis of MB under UV light is negligible and that the degradation process is predominantly driven by photocatalytic reactions occurring on the catalyst surface.

The superior activity of the catalyst can be attributed to the synergistic combination of semiconductor $CaFe_2O_4$ and conductive SWCNT, which together improve adsorption, charge separation, and radical generation.

The degradation kinetics of MB were analyzed using the pseudo-first-order Langmuir–Hinshelwood model:

$$\ln (C_0/C_t) = kt$$

where $k$ is the apparent rate constant.

The linear plot of $\ln (C_0/C_t)$versus irradiation time confirmed that the degradation process follows pseudo-first-order kinetics. The calculated rate constants were:

- $CaFe_2O_4$/SWCNT: 0.01005 $min^{-1}$
- Light only: 0.00078 $min^{-1}$

The catalytic rate constant was approximately 12.9 times higher than that of the light-only system, indicating a significant enhancement in reaction rate due to the presence of the nanocomposite.

The higher kinetic constant suggests faster generation of reactive oxygen species and more efficient electron transfer in the catalytic system.

## 5. Discussion

The results obtained in the present study clearly demonstrate that the incorporation of SWCNT into $CaFe_2O_4$ significantly enhances the optical and photocatalytic properties of the resulting nanocomposite. The UV–Visible spectra showed that while pristine SWCNT exhibited a characteristic absorption peak at 291 nm due to $\pi \rightarrow \pi^*$ transitions of the graphitic carbon framework, the $CaFe_2O_4$/SWCNT composite displayed an additional band around 360 nm and an extended absorption tail in the visible–NIR region. This broadened optical response indicates improved photon harvesting and strong interfacial electronic coupling between the ferrite phase and nanotube network. Such behavior has also been reported for $CaFe_2O_4$/g-$C_3N_4$/CNT composites, where enhanced visible-light absorption led to superior photocatalytic activity compared with pure $CaFe_2O_4$ [20]. Similar red-shifted absorption behavior has been observed in $ZnFe_2O_4$/CNT and $CoFe_2O_4$/CNT systems, where CNT incorporation improved light utilization and reduced recombination losses [21,22]. The FTIR results further confirmed successful composite formation through the coexistence of carbon-related functional groups and Fe–O/Ca–O lattice vibrations. The presence of surface hydroxyl groups is particularly important because they serve as precursors for hydroxyl radicals during irradiation. Comparable FTIR observations have been reported for $MgFe_2O_4$/CNT and ferrite-carbon hybrids, where strong oxide–carbon interfacial contact promoted efficient electron migration [23,24]. The photocatalytic degradation experiments revealed that the $CaFe_2O_4$/SWCNT nanocomposite achieved 79.9% degradation of methylene blue after 120 min, whereas only 8.9% degradation occurred under light-only conditions. The gradual decline of the MB absorption peak at 662 nm, accompanied by visible decolorization of the solution, confirms effective destruction of the dye chromophore. This large difference between catalytic and non-catalytic systems verifies that direct photolysis is negligible and that the catalyst is responsible for the major oxidation pathway. Comparable dye removal efficiencies have been reported for ferrite-based nanocomposites in previous studies. Liu et al. reported highly efficient degradation of organic pollutants using $CaFe_2O_4$/g-$C_3N_4$/CNT heterostructures under visible light [20], while Varghese et al. achieved nearly complete MB degradation using CuO/$CoFe_2O_4$/MWCNT ternary composites due to synergistic heterojunction effects [25]. Although ternary systems may show higher efficiencies, they often require more complex synthesis procedures and multiple optimization steps. In contrast, the present binary $CaFe_2O_4$/SWCNT system provides substantial degradation performance through a comparatively simple preparation route. The observed activity can be attributed to the high surface area of SWCNT, which increases adsorption of MB molecules near catalytic sites, and the narrow band gap of $CaFe_2O_4$, which allows efficient photoexcitation under irradiation [26,27]. The kinetic analysis provided further support for the

Journal of Chemical Health Risks

www.jchr.org

JCHR (2026) 16(3), 268-275 | ISSN:2251-6727

enhanced catalytic performance. The degradation process followed pseudo-first-order kinetics with an apparent rate constant of 0.01005 $min^{-1}$ for $CaFe_2O_4$/SWCNT, which was approximately 12.9 times higher than the light-only system (0.00078 $min^{-1}$). This strong kinetic enhancement indicates rapid generation of reactive oxygen species and improved charge separation in the nanocomposite. Similar rate enhancements have been reported for $CoFe_2O_4$/CNT and $TiO_2$/CNT photocatalysts, where CNTs acted as electron acceptors and conductive channels that prolonged charge carrier lifetime [28,29]. Mechanistically, upon irradiation, $CaFe_2O_4$ generates electron–hole pairs; electrons are transferred to SWCNT and react with dissolved oxygen to produce superoxide radicals ($\bullet O_2^-$), while holes generate hydroxyl radicals (•OH) from water or hydroxide ions. These radicals subsequently attack the aromatic structure of MB, leading to decolorization and mineralization. Such a mechanism is consistent with the established behavior of CNT-modified semiconductor photocatalysts [30–32]. Overall, the present findings confirm that $CaFe_2O_4$/SWCNT nanocomposites are promising low-cost photocatalysts for wastewater treatment and can compete favorably with more complex oxide-based systems reported in the literature [33,34].

## 6. Conclusion

Within the limitations of this study, a $CaFe_2O_4$/SWCNT nanocomposite was successfully synthesized and evaluated as an efficient photocatalyst for the degradation of methylene blue (MB) dye under UV irradiation. UV–Visible and FTIR analyses confirmed successful composite formation, enhanced light absorption, and strong interaction between $CaFe_2O_4$ and SWCNT. Overall, the $CaFe_2O_4$/SWCNT nanocomposite shows strong potential as a low-cost and effective photocatalyst for wastewater treatment and environmental remediation.

## References

1. Forgacs E, Cserháti T, Oros G. Removal of synthetic dyes from wastewaters: a review. Environ Int. 2004;30(7):953–71.
2. Robinson T, McMullan G, Marchant R, Nigam P. Remediation of dyes in textile effluent: a critical review. Bioresour Technol. 2001;77(3):247–55.
3. Yaseen DA, Scholz M. Textile dye wastewater characteristics and constituents of synthetic effluents: a critical review. Int J Environ Sci Technol. 2019;16:1193–226.
4. Khataee A, Kasiri MB. Photocatalytic degradation of organic dyes in the presence of nanostructured titanium dioxide: influence of operational parameters. J Mol Catal A Chem. 2010;328(1–2):8–26.
5. Wainwright M, Crossley KB. Methylene Blue—a therapeutic dye for all seasons? J Chemother. 2002;14(5):431–43.
6. Crini G. Non-conventional low-cost adsorbents for dye removal: a review. Bioresour Technol. 2006;97(9):1061–85.
7. Fujishima A, Zhang X, Tryk DA. $TiO_2$ photocatalysis and related surface phenomena. Surf Sci Rep. 2008;63(12):515–82.
8. Hoffmann MR, Martin ST, Choi W, Bahnemann DW. Environmental applications of semiconductor photocatalysis. Chem Rev. 1995;95(1):69–96.
9. Chong MN, Jin B, Chow CWK, Saint C. Recent developments in photocatalytic water treatment technology: a review. Water Res. 2010;44(10):2997–3027.
10. Yadav N, Ahmaruzzaman M. Recent advancements in $CaFe_2O_4$-based composite: properties, synthesis, and multiple applications. Energy Environ. 2024. doi:10.1177/0958305X231155491.
11. Blösser A. Nanostructured, single-phase ferrite materials: synthesis, characterization, and suitability for photocatalytic applications. University of Bayreuth; 2021.
12. Malik AQ, Singh H, Kumar A, et al. An overview on magnetic separable spinel as promising materials for photocatalysis and wastewater treatment. ES Energy Environ. 2022;8:44–67.
13. Alqassem B, Banat F, Palmisano G, Abu Haija M. Emerging trends of ferrite-based nanomaterials as photocatalysts for environmental remediation: a review. Sustain Mater Technol. 2024;39:e00873.
14. Iijima S. Helical microtubules of graphitic carbon. Nature. 1991;354:56–8.

Journal of Chemical Health Risks

www.jchr.org

JCHR (2026) 16(3), 268-275 | ISSN:2251-6727

15. Dai H. Carbon nanotubes: opportunities and challenges. Surf Sci. 2002;500(1–3):218–41.

16. Liu F, Dong S, Zhang Z, Li X, Dai X, Xin Y, et al. Synthesis of a well-dispersed $CaFe_2O_4$/g-$C_3N_4$/CNT composite towards the degradation of toxic water pollutants under visible light. RSC Adv. 2019;9:27874–84.

17. Foot PJ, et al. $MgFe_2O_4$/CNTs nanocomposite: synthesis, characterization, and photocatalytic activity. Int J Ind Chem. 2016;7:1–12.

18. Varghese D, et al. Synergistic design of CuO/$CoFe_2O_4$/MWCNTs ternary nanocomposite for enhanced photocatalytic degradation under visible light. Sci Rep. 2025;15:82926.

19. Kumar SG, Devi LG. Review on modified $TiO_2$ photocatalysis under UV/visible light: selected results and related mechanisms. J Phys Chem A. 2011;115(46):13211–41.

20. Liu F, Dong S, Zhang Z, Li X, Dai X, Xin Y, et al. Synthesis of a well-dispersed $CaFe_2O_4$/g-$C_3N_4$/CNT composite towards the degradation of toxic water pollutants under visible light. RSC Adv. 2019;9:27874–27884.

21. Wang Y, Zhang H, Li X, Chen J. $ZnFe_2O_4$/carbon nanotube hybrid photocatalysts with enhanced visible-light activity. Appl Surf Sci. 2017;392:45–53.

22. Kumar R, Singh P, Sharma A. $CoFe_2O_4$/CNT nanocomposites for photocatalytic dye degradation. J Mater Sci Mater Electron. 2018;29:11245–11254.

23. Foot PJ, et al. $MgFe_2O_4$/CNTs nanocomposite: synthesis, characterization, and photocatalytic activity. Int J Ind Chem. 2016;7:1–12.

24. Alqassem B, Banat F, Palmisano G, Abu Haija M. Emerging trends of ferrite-based nanomaterials as photocatalysts for environmental remediation. Sustain Mater Technol. 2024;39:e00873.

25. Varghese D, Nair SR, Joseph SJ, et al. Synergistic design of CuO/$CoFe_2O_4$/MWCNTs ternary nanocomposite for enhanced photocatalytic degradation under visible light. Sci Rep. 2025;15:82926.

26. Yadav N, Ahmaruzzaman M. Recent advancements in $CaFe_2O_4$-based composite: properties, synthesis, and multiple applications. Energy Environ. 2024. doi:10.1177/0958305X231155491.

27. Hoffmann MR, Martin ST, Choi W, Bahnemann DW. Environmental applications of semiconductor photocatalysis. Chem Rev. 1995;95(1):69–96.

28. Singh J, Verma A, Kumar S. Kinetic study of methylene blue degradation using magnetic $CoFe_2O_4$/CNT photocatalyst. Mater Chem Phys. 2020;244:122683.

29. Yu J, Yu H, Cheng B, Zhao X. Enhanced photocatalytic activity of $TiO_2$ powder by addition of carbon nanotubes. J Photochem Photobiol A Chem. 2006;182:121–127.

30. Khataee A, Kasiri MB. Photocatalytic degradation of organic dyes in the presence of nanostructured $TiO_2$: influence of operational parameters. J Mol Catal A Chem. 2010;328:8–26.

31. Dai H. Carbon nanotubes: opportunities and challenges. Surf Sci. 2002;500:218–241.

32. Fujishima A, Zhang X, Tryk DA. $TiO_2$ photocatalysis and related surface phenomena. Surf Sci Rep. 2008;63:515–582.

33. Ong CB, Ng LY, Mohammad AW. A review of ZnO nanoparticles as solar photocatalysts. Renew Sustain Energy Rev. 2018;81:536–551.

34. Wang X, Maeda K, Thomas A, Takanabe K, Xin G, Carlsson JM, et al. A metal-free polymeric photocatalyst for hydrogen production under visible light. Nat Mater. 2009;8:76–80.